TREATMENT OF NATURAL GAS WITH ZEOLITES

I. HANNUS, A. ÁDÁSZ–SZŰCS¹, I. KIRICSI, GY. TASI, F. BERGER,

J. HALÁSZ and P. FEJES

Institute of Applied Chemistry, Attila József University,

Rerrich Béla tér 1., H–6720 Szeged, Hungary

¹Great Plain Oil and Natural Gas Company, Szeged, Hungary

NATURAL GAS CLEANING INVOLVING THE REMOVAL OF H_2O AND H_2S IMPURITIES AND MINIMIZATION OF THE CO_2 CONTENT, IS VERY IMPORTANT FROM BOTH ENVIRONMENTAL AND ECONOMIC ASPECTS. LITERATURE DATA INDICATE THAT ZEOLITES WOULD BE EFFECTIVE IN THE SOLUTION OF THIS PROBLEM. OUR LABORATORY AND EXPERIMENTAL RESULTS SUPPORT THIS PERCEPTION. DIFFERENT NATURAL AND SYNTHETIC ZEOLITES WERE COMPARED IN THE ADSORPTION PROCESS BY MEANS OF X–RAY, INFRARED, DERIVATOGRAPHIC AND GAS CHROMATOGRAPHIC TECHNIQUES.

Introduction

Zeolites, as excellent selective adsorbents compared with silica gel and activated carbon (see Figure 1), are useful for many phases of natural gas treatment [1].

Drying was the most obvious initial application for zeolites in the natural gas industry. With the classical method (glycol injection) it was possible to attain a dew point of 233 K (–40 ⁰C), but with zeolites dew point of lower than 203 K (–70 ⁰C) can be achieved easily and economically. The first installations were made in the late fifties and the early sixties in the United States [2–4].

Gas sweetening is the other important field of natural gas treatment in general, including Hungarian natural gas sources [5]. Among the different acidic components, mercaptans are the most strongly adsorbed sulphur compounds, followed by H_2S, and CO_2 is the most weakly adsorbed component in this series.

If the purpose is to remove only H_2O and CO_2 impurities, the task can be solved relatively easily (see Figure 2) [6].
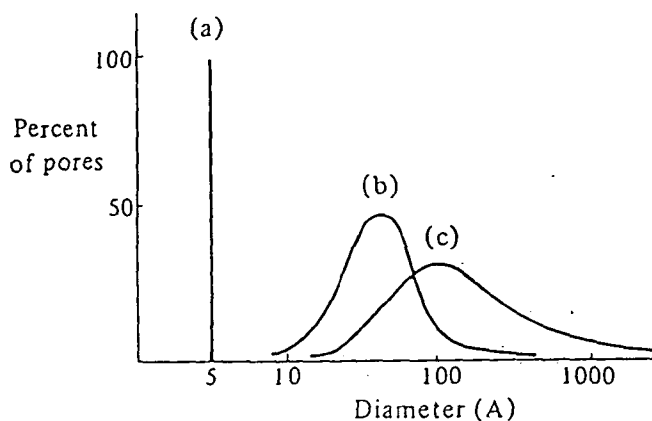

Figure 1:   Distribution of pore sizes in microporous adsorbent (a) Dehydrated zeolite, *e.g.* type A, (b) typical silica gel, (c) activated carbon (from *ref.* [1]).

Various natural gases contain H_2S in different amounts; in some cases its content can reach 25% [7]. It is possible to dry such strongly acidic natural gases with zeolites and to remove the sulphur content with large—pore X—type zeolites [8].

It is a complex problem to remove the H_2O and H_2S impurities from a CO_2—rich natural gas and also to reduce the CO_2 content. An effective solution can be found in the literature: a mixed adsorption and absorption method [3]. In some cases, also the deep—cooling absorption process can be useful [9].

In this work we report laboratory results obtained with a natural gas of Hungarian origin, where the aims were to remove H_2O and H_2S impurities and to minimize the CO_2 using Hungarian natural zeolites and different Hungarian—made synthetic zeolites.
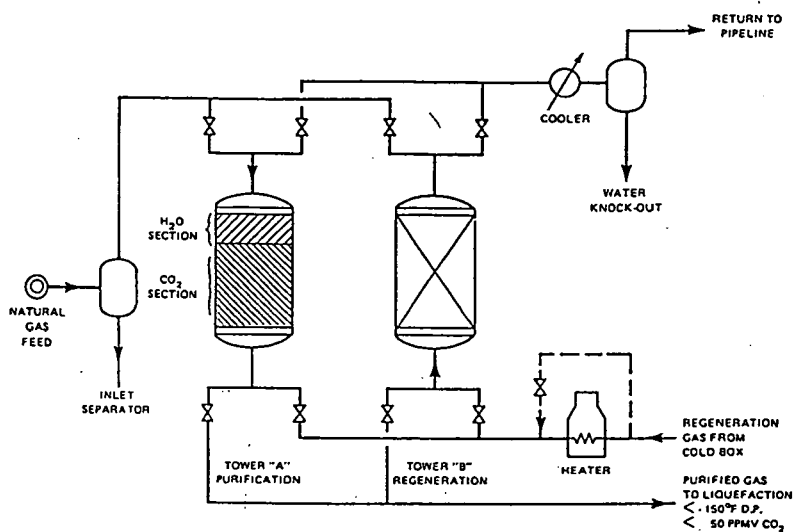
Figure 2: Zeolite adsorption system for combined natural gas dehydration and CO_2 removal (from *ref.* [6])
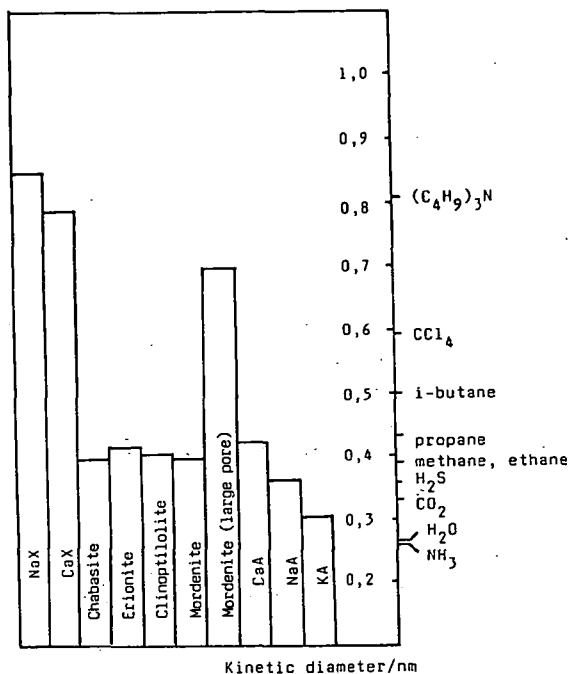
Experimental

Materials

The natural zeolites used in the experiments were from the Hegyalja Works of Hungarian Ore and Mineral Mines. Samples M_{30}, M_{70} and M_{80} contained 30, 70 and 80% mordenite, respectively. Zeolite ERSORB–4 was a product of Erdőkémia (Forest Chemistry) Co. and contained clinoptilolite.

Among the synthetic zeolites, we used Na–mordenite (Norton Co.), Linde 4A, 5A and 13X (Union Carbide Corporation), NaA zeolite (Merck) and Hungarian–made NaA. (Figure 3 illustrates the pore sizes of the different zeolites, as compared with the kinetic diameters of simple molecules.)

The natural gas used in the adsorption experiments was from the Algyö

gas—field, near Szeged, in South Hungary.

Figure 9 and axis labels:

- 1,0
- 0,9
- 0,8 — $(C_4H_9)_3N$
- 0,7
- 0,6 — CCl_4
- 0,5 — i-butane
- 0,4 — propane / methane, ethane / H_2S / CO_2
- 0,3 — H_2O / NH_3
- 0,2

Bar labels: NaX, CaX, Chabasite, Erionite, Clinoptilolite, Mordenite, Mordenite (large pore), CaA, NaA, KA

Kinetic diameter/nm

Figure 9:   Pore sizes of different zeolites compared with kinetic diameters of simple molecules

Methods

The zeolite contents of the natural zeolites were determined by X—ray diffraction analysis at ambient temperature with a DRON—3 diffractometer.

The water contents of the samples were determined with a MOM—Q derivatograph, in ceramic crucibles, at a heating rate of 10 degree/min.

For the KBr pellet infrared technique, a SPECORD—75 IR spectrophotometer

was utilized. In each case, the spectra of wafers of 1 wt% zeolite in KBr were recorded vs. a standard KBr pellet.

In the adsorption experiments different methods were applied. The adsorption of CO_2 and CH_4 was investigated with a static method in volumetric adsorption equipment. The equipment and details of method were reported earlier [10].

In most of the adsorption investigations, a dynamic flow method was used, where either a thermal conductivity detector was applied for gas analysis or the volume of gas at the exit was measured directly [11]. In the industrial adsorption process, gaschromatographic analysis was used (CHROM—4 GC with a thermal conductivity detector).

Results and discussion

Laboratory investigations

Water adsorption

The water adsorption capacities of the samples were determined by derivatography. The pretreatment conditions were the same in every case, in order to obtain comparable results: equilibration in water vapour over saturated NH_4Cl solution for 2 days [12]. The weight losses of the different zeolites up to 1073 K are listed in Table I.

Figure 4 shows typical "water loss" curves for an "A"—type zeolite. From the data in Table I, it is clear that synthetic zeolites have much larger adsorption capacities than their natural counterparts. In the case of natural zeolites, the amount of water adsorbed correlates well with the amount of the zeolitic phase in the minerals.

H_2S adsorption

H_2S adsorption was studied with the dynamic method. Figure 5 shows the

Table I

Weight losses of different zeolites up
to 1073 K, measured by thermogravimetry

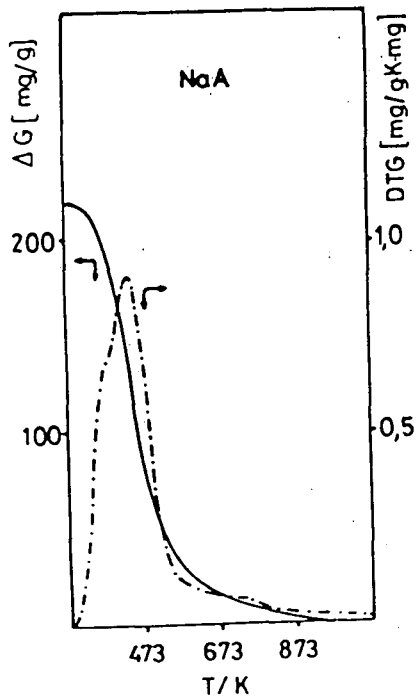| Zeolite	mg H_2O/g dry zeolite
Linde NaX	272
Linde 5A	238
Linde 4A	228
Merck NaA	197
Hung. NaA	163
Na—mordenite	150
M_{80}	117
M_{70}	111
M_{30}	63
ERSORB—4	89

Figure 4: Water loss curves of
zeolite NaA
TG curve ————
DTG curve — · — · —

experimental apparatus. Hydrogen was used as the carrier gas and H_2S was taken from a Kipp apparatus. The adsorbent was activated at 673 K in a system of flowing H_2 and the adsorption was carried out at room temperature. A thermal conductivity detector was used for gas analysis. Through measurement of the weight of the adsorbent column before and after the adsorption the adsorption capacity could be checked gravimetrically, too.
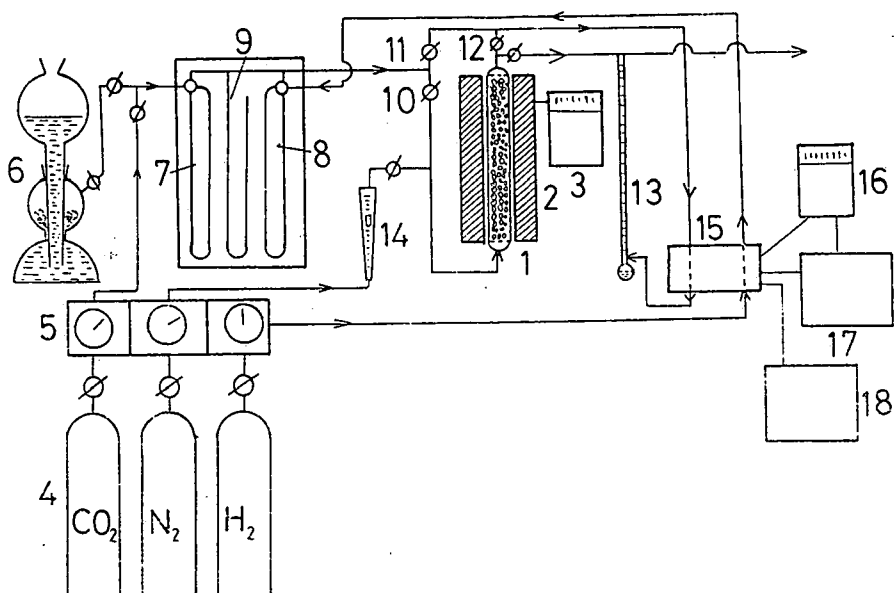
Figure 5:   Dynamic adsorption apparatus with thermal conductivity detector (1) adsorber; (2) heater; (3) regulator; (4) gas tanks; (5) pressure gauge; (6) Kipp apparatus; (7,8,9) manometers; (10,11,12) valves; (13) soap film meter; (14) flow meter; (15) thermal conductivity detector; (16) regulator; (17) battery; (18) recorder.

For example, in the case of natural mordenite M_{70}, we measured (by weight) the

adsorption capacity of 60 mg H_2S/g dry zeolite for a gas stream containing 10% H_2S and obtained the same value by the dynamic method.

The adsorption of H_2S from natural gas containing 100 ppm H_2S was investigated. Figure 6 shows the adsorption curve and the increase in the adsorbent temperature measured in the middle of the adsorption column. The relatively high temperature increase illustrates that H_2S adsorbs more strongly than CO_2.
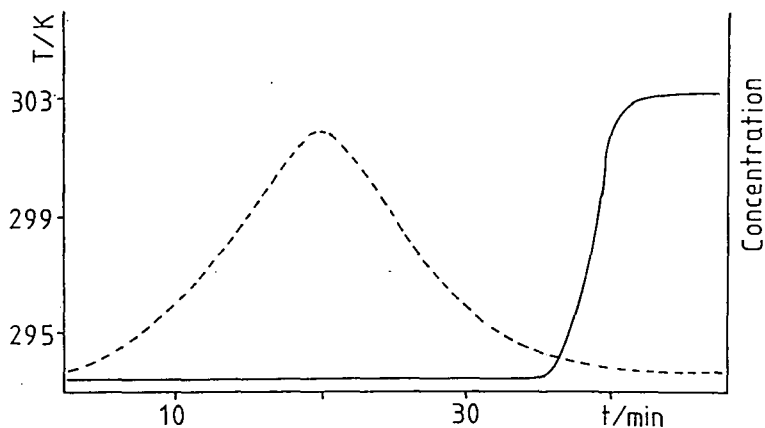

Figure 6:   Breakthrough curve of natural gas with H_2S and CO_2 content over zeolite 4A (————), temperature in middle of column (— — —)

CO₂ adsorption

1. With a static method

Figure 7 shows the adsorption isotherms of CO_2 and CH_4 on NaA (Merck) and Hungarian NaA. CH_4 is practically not adsorbed, due to the apolarity of the hydrocarbon molecule.

Adsorption isotherms measured at different temperatures can be described by the well–known Langmuir equation. The experimental and theoretical results are similar.

The adsorption capacity of the Hungarian—made NaA proved to be 40% lower than that of the Merck NaA.
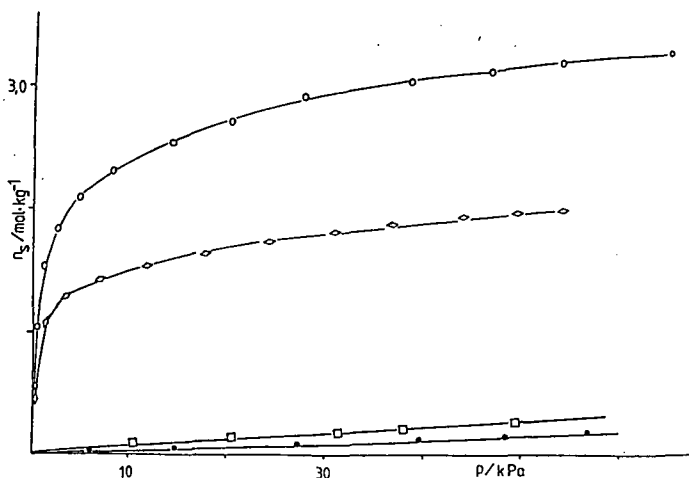

Figure 7:   Adsorption isotherms of CO_2 and CH_4 at 298 K
CO_2 over Merck NaA (o); CO_2 over Hungarian NaA (◇);
CH_4 over Merck NaA (□); CH_4 over Hungarian NaA (•)

2. With a dynamic method using a thermal conductivity detector

   a. CO_2 adsorption from a H_2 stream

In these experiments, the CO_2 content was adjusted to 10%, which was similar to that in natural gas. During the adsorption, the temperature was measured in the adsorption column. The maximum increase in temperature due to the adsorption of CO_2 was about 6 degrees, showing a relatively weak adsorption of CO_2. Under similar conditions, H_2S adsorption caused a rise in temperature of about 8—10 degrees (see Figure 6).

The amount of CO_2 adsorbed (A) was calculated from the material balance equation [11]:

$$A = c_0(tw - V_h)$$

where c_0 = concentration of CO_2, t = time of breakthrough, w = flow rate, V_h = dead volume.

The specific adsorption capacity (a) was calculated from A. The experimental results are given in Table II. The calculated specific adsorption capacity and the gravimetrically measured data are in good agreement. The highest adsorption capacity was measured for synthetic zeolite 5A.

Table II

CO_2 adsorption from a H_2 stream

Zeolite	Loading (g)	V flow rate (cm³/min)	$c^0_{CO_2}$ (%)	t/breakthrough time (min)	a/spec.ads. amount from t (mg/g)	gravi.
M$_{30}$	4.75	33.2	9.64	30	35.8	42.1
M$_{70}$	4.35	33.1	9.67	32	45.9	57.5
M$_{80}$	4.78	33.6	10.9	30	41.0	46.1
ER–SORB–4	4.9	33.4	10.9	31	50.6	47.1
LINDE 4A	4.7	32.1	10.9	66	84.1	85.0
LINDE 5A	4.9	32.9	8.8	80	104.1	107.1
HUNG. NaA	4.9	31.1	9.9	61	67.3	62.0

b. CO_2 adsorption from natural gas

In these experiments we used natural zeolite M$_{70}$ (exhibiting the greatest adsorption capacity) and synthetic zeolites 4A and 5A. Table III shows the results. For

zeolites M_{70} and 4A, the specific adsorbed amounts were similar to those obtained from H_2 stream in the previous experiment, but for zeolite 5A the adsorption was found to be higher. In agreement with literature data, the reason is that the hydrocarbons of natural gas can adsorb in the larger pores of 5A (see Figure 3).

The breakthrough curve in Figure 8 supports this explanation, because a multistep curve was obtained over 5A instead of the smooth curves observed over natural zeolites and synthetic 4A.

3. CO_2 adsorption by measuring the gas volume leaving the column

The theoretical and experimental aspects of this technique were described by Fejes [11]. The schematic outline of the apparatus is shown in Figure 9.

The advantages of the soap film volume meter are as follows:

— the apparatus is simpler than that with a thermal conductivity detector (TCD)

— it is not necessary to determine the dead volume of the column in a separate experiment,

Table III

CO_2 adsorption from natural gas

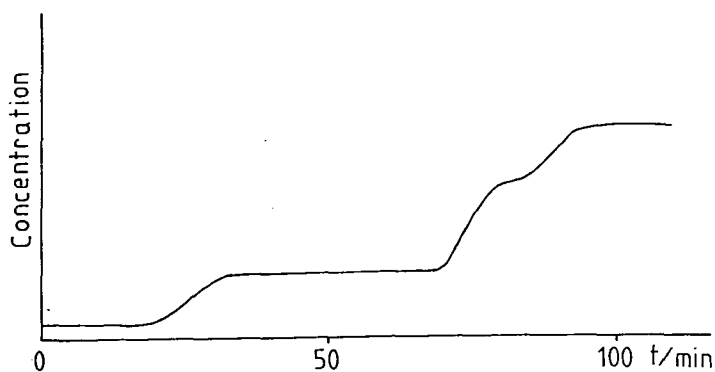| Zeolite	Loading (g)	V flow rate (cm³/min)	t/breakthrough time (min)	a/specific ads. amount (mg/g)	regeneration
M_{70}	5.1	31.6	—	49	673 K in H_2
M_{70}	5.1	32.0	38	49	673 K in H_2
5A	4.0	32.0	90	150	673 K in H_2
5A	4.0	31.6	92	150	673 K nat. gas
4A	4.1	31.6	44	85	673 K nat. gas
4A	2.05	30.0	45	82	473 K nat. gas

Figure 8: Breakthrough curve of CO_2 from natural gas over zeolite 5A
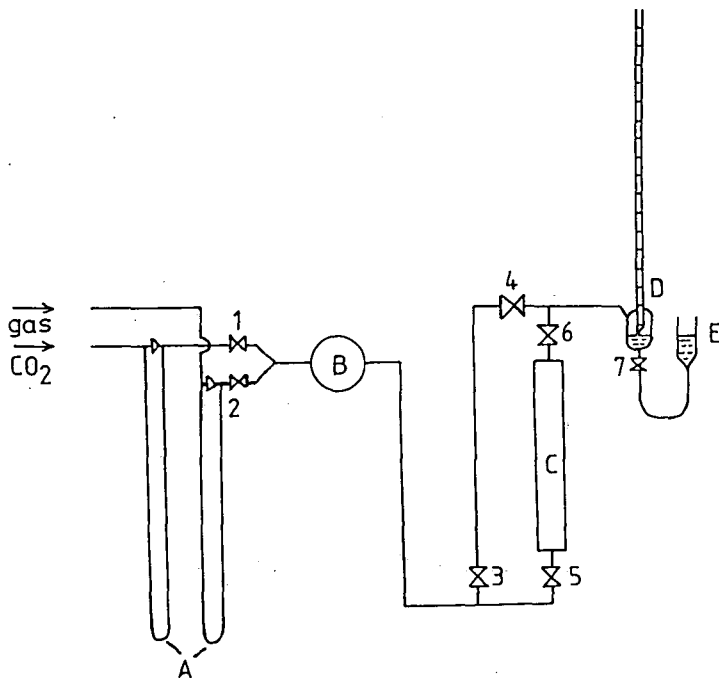

Figure 9:   Dynamic adsorption apparatus with soap film meter

A: differential manometers; B: gas mixing vessel; C: adsorption column; D: soap film meter; E: liquid level regulator; 1–7: valves

— the experimental error is less than that in the case of TCD.

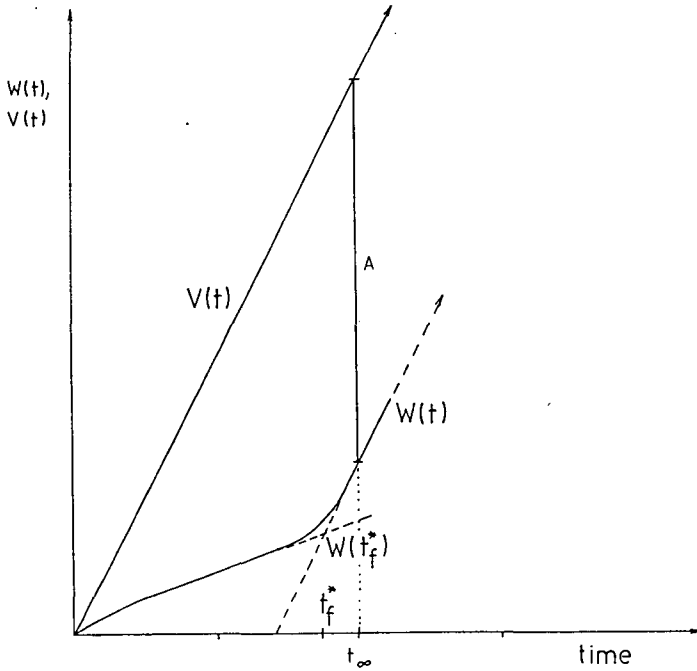Measurement of the flow at the outlet in time, $W(t)$, gave the characteristic curve shown in Figure 10.

Figure 10: Determination of adsorption amount from dynamic measurements

$V(t)$ is the flow at the inlet which is assumed to depend linearly on time. The difference between $V(t)$ and $W(t)$ at an appropriately chosen time, t, gives the equilibrium sorbed amount (A) [11]:

$$A = Lma_0 = V(t) - W(t)$$

where L = length of column,

m = mass of adsorbent per unit length,

a_0 = adsorbed amount per unit mass relating to inlet concentration, x_0.

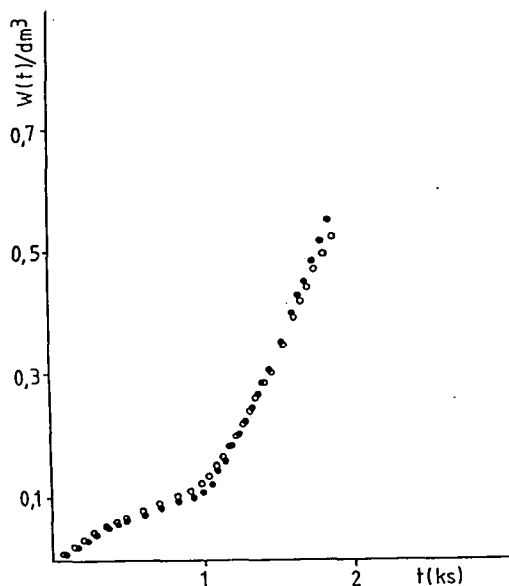This technique proved to be suitable due to its surprisingly good reproducibility (Figure 11).

Figure 11: Reproducibility of measurements

Table IV shows the characteristic data on the columns used.

In the first series of experiments, the adsorption of pure CO_2 was measured at different flow rates with column 1. The conclusion to be drawn from the results is plausible: the smaller the flow rate, the greater the effective adsorption. The equilibrium adsorbed amounts, of course, are independent of the flow rate at t.

Figure 12 shows the results obtained with natural gas–CO_2 mixtures at different flow rates with column 2.

With adsorption column 3, the best result was observed at the smallest flow rate (2.41 mmol/g). This value is lower than that measured with the static method (3.33 mmol/g).

Table IV

Characterization of columns

No.	Length (cm)	Inner diameter (cm)	Volume (cm³)	Loading (g)	Mass per unit length (g/cm)
1	16	0.9	10.1	7.5	0.5
2	20	2.2	75.9	47.0	2.35
3	18	1.5	31.8	24.5	1.36
4	29	1.5	51.2	36.0	1.24

Figure 13 shows the adsorption curves for adsorption column 4 filled with Hungarian–made NaA (a) and Merck NaA (b). The adsorption capacity of Merck NaA exceeds that of Hungarian–made NaA by a factor of 2. The results are given in Table V.

Table V

Results obtained from CO_2 adsorption by measuring gas volume leaving column

No.	Diameter of column (cm)	Mass of adsorbent (g)	Mass per unit length (g)	Inlet flow rate (cm³/min)	CO_2 conc. x_0	Ads. CO_2 (cm³)	Breakthrough time (min)
1	0.9	7.7	0.48	13.5	1.0	389	28.5
2	2.2	47.0	2.35	86.0	1.0	1040	21.3
3	2.2	47.4	2.37	50.0	0.9	380	13.3
4	2.2	47.2	2.36	35.7	0.86	1160	75.0
5	1.5	24.4	1.36	60.0	0.75	200	8.7
6	1.5	24.4	1.36	27.9	0.47	1320	75.0
7	1.5	35.5	1.22	60.0	0.75	1200	52.0
8	1.5	35.5	1.22	60.0	0.8	1480	52.0
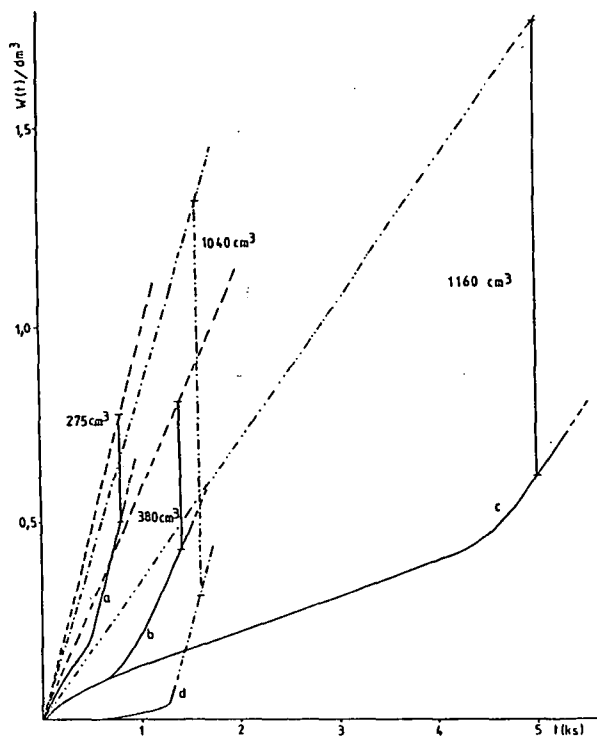
Figure 12:   Breakthrough curves of CO_2 from gas mixture in column 2

a: $dV/dt = 88$ cm^3/min; $x^0_{CO_2} = 0.77$ cm^3/cm^3

b: $dV/dt = 50$ cm^3/min; $x^0_{CO_2} = 0.90$ cm^3/cm^3

c: $dV/dt = 36$ cm^3/min; $x^0_{CO_2} = 0.86$ cm^3/cm^3

d: $dV/dt = 86$ cm^3/min; $x^0_{CO_2} = 1.00$ cm^3/cm^3

The reversibility of CO_2 adsorption

Samples of Merck and Hungarian zeolites were saturated with CO_2 previously and the CO_2 was desorbed overnight at room temperature and atmospheric pressure. Infrared investigations were carried out with the KBr pressed pellet technique to check the formation of CO_3^{2-} in the zeolite channels. For the Hungarian—made NaA, a

characteristic CO_3^{2-} peak could be observed in the spectrum at 1380 cm^{-1} (see Figure 14).

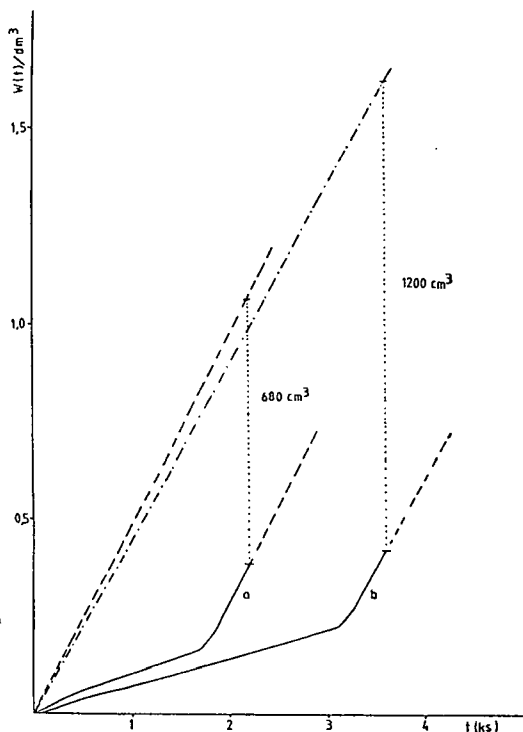*Figure 13:*   Breakthrough curves of CO_2 over Hung. NaA (a) and Merck NaA (b) zeolites in column 4 (dV/dt = 60 cm^3/min; $x^0_{CO_2}$ = 0.75 cm^3/cm^3).

This means that CO_2 adsorption is not reversible for the Hungarian–made NaA in contrast with the Merck NaA. When the two samples were suspended in distilled water (0.5 g, in 50 cm^3 water, with stirring for 2 hours), the pH of the aqueous phase was almost the same in the two cases.

It is presumed that CO_3^{2-} formation is due to the presence of Al_2O_3–hydrogel from incomplete NaA zeolite crystallization.
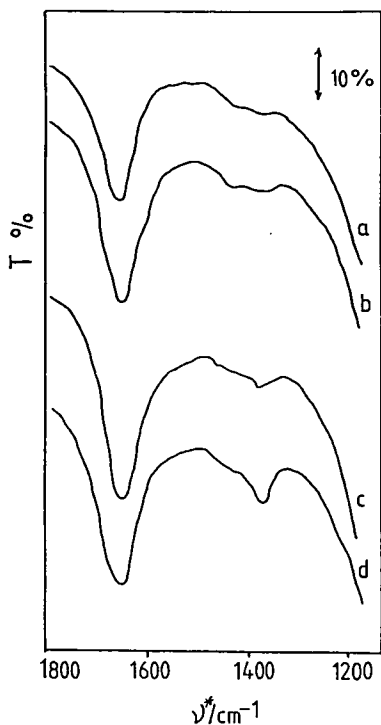
Figure 14:   Infrared spectra

a: Original Merck NaA;

b: after CO_2 adsorption;

c: original Hung. NaA;

d: after CO_2 adsorption.

4. CO_2 adsorption under semiadiabatic conditions

In a real industrial separation, the adsorption is an adiabatic process because of the large dimensions of the column. The heat of adsorption causes a temperature increase in the adsorbent. This is of some advantage from the aspect of the transport, but this beneficial effect is counterbalanced by a large decrease in adsorption capacity. The investigation of adsorption under adiabatic conditions is very important from an industrial point of view.

Figure 15 shows a high—pressure column used in semiadiabatic measurements. The temperature of the adsorbent was measured at the beginning and the end of the

column with thermocouples. The breakthrough of the adsorptive was detected with a soap film flow meter. Three types of zeolites (H–NaA, M–NaA and L–NaX) and pure CO_2 were used in these experiments. Typical temperature curves are shown in Figure 16 for CO_2 adsorption at atmospheric pressure. Activation of the zeolites was carried out at 673 K. The adsorbed amounts are markedly lower than the equilibrium values due to the liberation of adsorption heat.
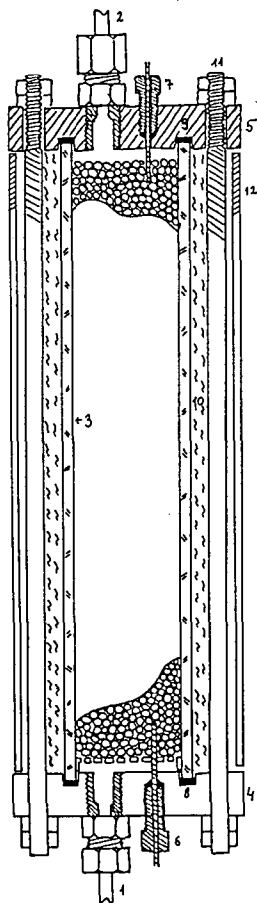
Figure 15:   High–pressure adsorption column for semiadiabatic measurements

(1) inlet; (2) outlet;

(3) glass tube;

(4,5) covering plates;

(6,7) thermocouples;

(8,9) teflon rings;

(10) heat insulation;

(11) holding bars;

(12) protecting tube

When regeneration was carried out in vacuo during 2 hours without heating, the adsorption capacity led to losses of 27, 23 and 11%, respectively, for zeolites H–NaA, M–NaA and L–NaX, as compared with samples regenerated at 673 K (see Table VI). On increase of the CO_2 pressure from 1 bar to 2.5 and 5 bars, the adsorbed amounts increased, too.
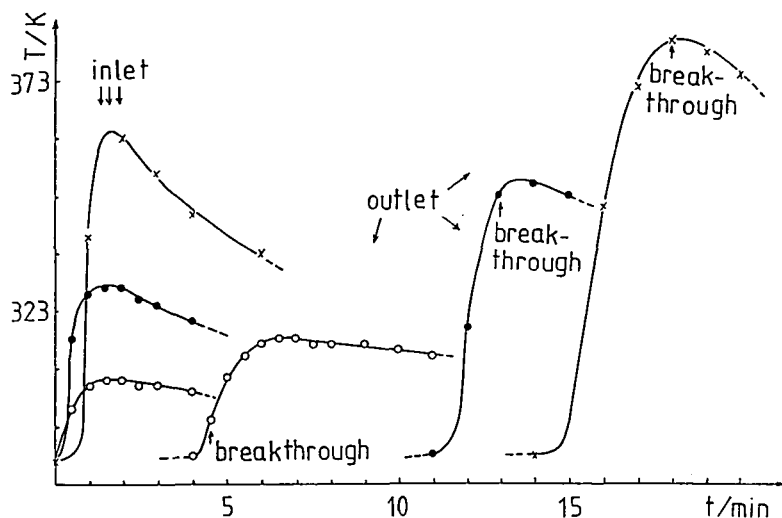

Figure 16: Semiadiabatic CO_2 adsorption; zeolites were actived at 673 K; p = 1 bar, W_{CO_2} = 0.5 dm³/min.

zeolite:	adsorbed CO_2:
Hung. NaA	0.59 mmol/g
Merck NaA	1.82 mmol/g
Linde NaX	2.78 mmol/g

Finally, the time of the desorption was decreased to 0.1 hour and the pressure to 0.1 bar. These conditions are similar to those in the industrial process when a pressure swing cycle is applied. The last row of Table VI shows the amount of CO_2 adsorbed.

The conclusion is that NaA is suitable for cleaning natural gases rich in CO_2, nevertheless, faujasites (NaX, NaY) are superior, because of their greater capacity and easy regeneration.

Table VI

Semiabiabatic CO_2 adsorption on three different zeolites under different

pretreatment and adsorption conditions

Zeolite	Pretreatment	Pressure/bar	CO_2 mmol/g zeolite
H–NaA M–NaA L–NaX	at 673 K in vacuo 2 hours	1.0	0.59 1.82 2.78
H–NaA M–NaA L–NaX	at room temp. in vacuo 2 hours	1.0	0.42 1.39 2.47
H–NaA M–NaA L–NaX	at room temp. in vacuo 2 hours	2.5	0.59 1.44 2.98
H–NaA M–NaA L–NaX	at room temp. in vacuo 2 hours	5.0	0.65 1.48 3.42
H–NaA M–NaA L–NaX	at room temp. 0.1 bar 0.1 hours	5.0	– 0.61 1.74

Industrial investigations

The experimental set–up is shown in Figure 17.

The adsorber was filled with zeolite 4A. Gas samples at the inlet and outlet were analysed with a CHROM–4 gaschromatograph. In a typical experiment, the adsorbent filling was 1.7 kg, the pressure at the inlet was 50 bar and the flow rate of

the outlet, purified gas was 700 dm³/hr at atmospheric pressure. The analytical data are shown in Table VII. Figure 18 depicts the breakthrough curve for CO_2.

If the requirement is to attain 0.5% CO_2 in the outlet gas, the breakthrough time is about 1.25 hr; this means in other words that about 0.5 m³ gas can be purified per kg adsorbent per cycle. Under these conditions the adsorption capacity for CO_2 is 0.16 kg/kg zeolite. In the laboratory experiment, 0.13 kg CO_2/kg zeolite was measured at 1 bar.
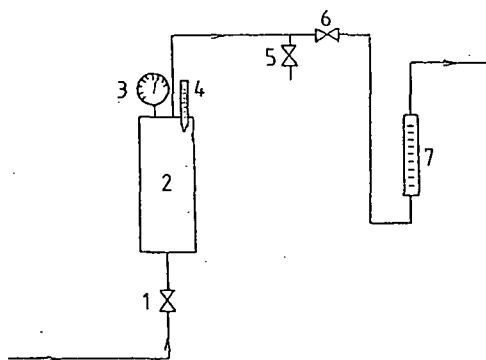

Figure 17:   Industrial adsorption apparatus

(1,6) regulating valves;   (2) adsorber;   (3) pressure   gauge; (4) thermometer; (5) blow—off valve; (7) flow meter

Conclusions

On the basis of literature data and the present results, it was shown that CO_2 can be removed from CO_2—rich natural gases effectively and economically by using adsorption techniques with zeolites as adsorbents.

Moreover, zeolites are the only adsorbents which are effective enough to solve this problem.

When zeolites NaA and NaX are compared for this task, NaX clearly surpasses NaA because of its greater adsorption capacity and easy regenerability.

Table VII

Typical analysis set from an industrial adsorption

Component	Time/hr										
	0.0	0.25	0.6	1.6	2.3	2.85	3.3	3.85	4.3	4.85	5.3
C_1	81.96	93.94	93.62	89.43	84.58	83.59	83.03	82.81	82.64	83.04	82.42
C_2	4.12	2.92	3.54	4.34	4.16	4.14	4.40	4.31	4.26	4.01	3.95
C_3	1.56	1.98	1.72	1.67	1.56	1.57	1.60	1.55	1.58	1.55	1.71
C_4	0.44	0.86	0.74	0.67	0.61	0.66	0.58	0.53	0.53	0.66	0.67
C_5	0.36	0.64	0.34	0.22	0.32	0.37	0.28	0.24	0.23	0.15	0.29
H_2O+H_2S	1.32	–	–	–	0.18	0.17	0.10	0.49	0.35	0.40	0.38
CO_2	10.31	–	–	3.64	8.58	9.50	10.01	10.14	10.41	10.19	10.58
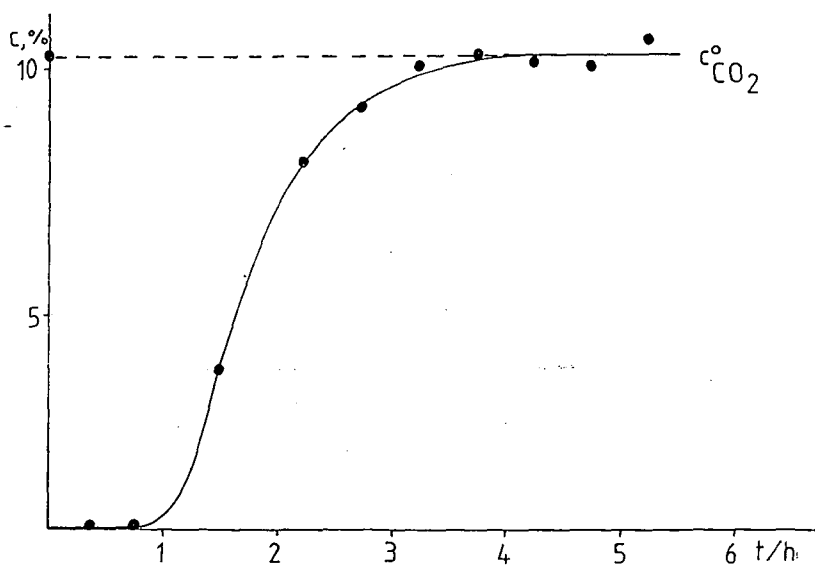
Figure 18: Breakthrough curve of CO_2 in an industrial experiment

References

[1]   *Breck, D. W.*: Zeolite Molecular Sieves, J. Wiley,

Interscience Publication, 1974.

[2] *Clark, E. L.*: Oil and Gas J., 57, 120 (1959).

[3] *Thomas, T. L., E. L. Clark*: Oil and Gas J., 65, 112 (1967).

[4] *Collins J. J.*: Chem. Eng. Prog., 66, 66 (1968).

[5] *Csákó D., L. Pető, P. Valastyán*: Kőolaj és Földgáz, 18, 353 (1985).

[6] *Anderson, A.*: ACS Symp. Ser., 40., 637 (1977).

[7] *Kraychy, P. N., A. Masuda*: Oil and Gas J., 64, 66 (1966).

[8] *Karge, H. G., J. Raskó*: J. Colloid Interface Sci., 64, 522 (1978).

[9] *Kulijev, A. M., P. D. Sihalizade, P. Valastyán*: Kőolaj és Földgáz, 14, 321 (1981).

[10] *Kiricsi, I., Gy. Tasi, H. Förster, P. Fejes*: Acta Phys. et Chem. Szeged, 33, 69 (1987).

[11] *Fejes, P.*: Dissertation, 1964.

[12] *Hannus, I., I. Kiricsi, P. Fejes*: Magy. Kém. Lapja, 39, 430 (1984).

ОБРАБОТКА ЕСТЕСТВЕННОГО ГАЗА ЦЕОЛИТАМИ

И.ГАННУШ, А.АДАС—СЮЧ, И.КИРИЧИ, ДЬ.ТАШИ, Ф.БЕРГЕР, Я.ГАЛАС, П.ФЕЕШ

На основании литературных и своих данных показано, что CO_2 эффективно и экономично может быть выделен из богатых CO_2 содержанием естественных газов с применением адсорбционной техники на цеолитах. Больше того, можно сказать, что цеолиты являются единственным видом адсорбентов, которые достаточно эффективны для разрешения этой проблемы. При сравнении применимости цеолитов NaA и NaX для этой цели, NaX значительно превосходит NaA тип, вследствие более значительной адсорбционной емкости и легкой регенерируемости.